

ppi 201502ZU4659

Esta publicación científica en formato digital es
continuidad de la revista impresa

ISSN 0254 -0770 / e-ISSN 2477-9377 / Depósito legal pp 197802ZU38



REVISTA TÉCNICA

DE LA FACULTAD DE INGENIERÍA

Una Revista Internacional Arbitrada
que está indizada en las publicaciones
de referencia y comentarios:

- REDALYC
- REDIB
- SCIELO
- DRJI
- INDEX COPERNICUS INTERNATIONAL
- LATINDEX
- DOAJ
- REVENCYT
- CHEMICAL ABSTRACT
- MIAR
- AEROSPACE DATABASE
- CIVIL ENGINEERING ABSTRACTS
- METADEX
- COMMUNICATION ABSTRACTS
- ZENTRALBLATT MATH, ZBMATH
- ACTUALIDAD IBEROAMERICANA
- BIBLAT
- PERIODICA

UNIVERSIDAD DEL ZULIA

Dr. Ignacio Rodríguez Iturbe - Zuliano ilustre
Ingeniero civil, hidrólogo profesor universitario,
doctor honoris causa de la Universidad del Zulia,
epónimo de la orden al mérito Dr. Ignacio Rodríguez Iturbe,
ciudadano ejemplar con numerosos premios nacionales e internacionales.



Evaluation of the Isomerization of α -Pinene Epoxide to Campholenic Aldehyde Using a Catalyst Obtained from Orange Peels (*Citrus sinensis*)

Marta Mediavilla-Quintero^{1,2} , Aída Luz Villa^{2*} 

¹Facultad de Ingeniería, Universidad Central de Venezuela, UCV, P.O. Box 48.057, Caracas 1041-A, Venezuela

² Grupo de Investigación de Catálisis Ambiental, Departamento de Ingeniería Química, Facultad de Ingeniería, Universidad de Antioquia UdeA, Calle 70 No.52-21, Medellín, Colombia

*Corresponding author: aida.villa@udea.edu.co

<https://doi.org/10.22209/rt.v46a03>

Received: August 10, 2022 | Accepted: March 21, 2023 | Available: April 15, 2023

Abstract

Orange peels (*Citrus sinensis*) are an abundant lignocellulosic residue that can be used as a carbon source to obtain solids with catalytic potential in the transformation of terpenes and their oxides into value-added products. This research seeks to evaluate the isomerization of α -pinene epoxide to campholenic aldehyde using a catalyst obtained from orange peels. The material OAC-Zn was obtained by activation of orange peel with $\text{ZnSO}_4 \cdot 7\text{H}_2\text{O}$ followed by thermal treatment at 500 °C; an additional solid was obtained from orange peel by pyrolysis at 500 °C (OC-500). XRD revealed the presence of ZnO and ZnS in OAC-Zn; TGA analysis indicated thermal stability in OAC-Zn and OC-500 materials; SEM images showed porous surfaces of different morphology, and the presence of microporosity in OC-500 and mesoporosity in the OAC-Zn that was confirmed by physical nitrogen adsorption. The elements C, O, Zn and S were identified in OAC-Zn by EDX analysis. The results of TPD-NH₃ showed that the solids contained medium and weak acidity. Campholenic aldehyde was synthesized with a 96 % selectivity over the material OAC-Zn.

Keywords: carbon; mesoporous; terpenes; waste; XRD.

Evaluación de la Isomerización de Epóxido de α -Pino a Aldehído Canfolénico Utilizando un Catalizador Obtenido de Cáscaras de Naranja (*Citrus sinensis*)

Resumen

Las cáscaras de naranja (*Citrus sinensis*) son residuos lignocelulósicos abundantes que pueden ser utilizados como fuente de carbono para obtener sólidos con potencial catalítico en la transformación de terpenos y sus óxidos en productos de valor agregado. Esta investigación buscó evaluar la isomerización de óxido de α -pino a aldehído canfolénico, utilizando un catalizador obtenido de cáscaras de naranja. El material OAC-Zn se obtuvo por activación de las cáscaras con $\text{ZnSO}_4 \cdot 7\text{H}_2\text{O}$, seguido de tratamiento térmico a 500 °C; también se obtuvo un sólido de la pirólisis de la cáscara a 500 °C (OC-500). Mediante DRX se identificó la presencia de ZnO y ZnS en OAC-Zn; los análisis por TGA indicaron estabilidad térmica en OAC-Zn y OC-500; las imágenes SEM mostraron superficies

porosas de diferente morfología, así como la presencia de microporosidad en OC-500 y de mesoporosidad en OAC-Zn, que fueron confirmadas mediante adsorción física de nitrógeno. En los análisis EDX se identificaron los elementos C, O, Zn y S en OAC-Zn; los resultados de TPD-NH₃ mostraron que los sólidos contenían acidez media y débil. Se sintetizó aldehído canfolénico con selectividad de 96 % con el material OAC-Zn.

Palabras clave: carbón; DRX; mesoporos; residuo; terpenos.

Avaliação da Isomerização de α -Pineno Epóxido a Aldeído Campolênico Usando um Catalisador Obtido de Cascas de Laranja (*Citrus sinensis*)

Resumo

Cascas de Laranja (*Citrus sinensis*) são abundantes resíduos lignocelulósicos que podem ser utilizados como fonte de carbono para obtenção de sólidos com potencial catalítico na transformação de terpenos e seus óxidos em produtos de valor agregado. Esta pesquisa buscou avaliar a isomerização do óxido de α -pineno a aldeído canfolénico, utilizando um catalisador obtido a partir de cascas de laranja. O material OAC-Zn foi obtido pela ativação das cascas com ZnSO₄·7H₂O, seguida de tratamento térmico a 500 °C; um sólido também foi obtido a partir da pirólise da casca a 500 °C (OC-500). Através do DRX foi identificada a presença de ZnO e ZnS no OAC-Zn; As análises de TGA indicaram estabilidade térmica em OAC-Zn e OC-500; As imagens de SEM mostraram superfícies porosas de morfologia diferente, bem como a presença de microporosidade em OC-500 e mesoporosidade em OAC-Zn, que foram confirmadas por adsorção física de nitrogênio. Nas análises de EDX, os elementos C, O, Zn e S foram identificados em OAC-Zn; os resultados do TPD-NH₃ mostraram que os sólidos continham acidez média e fraca. Aldeído canfolénico foi sintetizado com uma seletividade de 96 % com o material OAC-Zn.

Palabras clave: carvão; DRX; mesoporos; residuo; terpenos.

Introduction

Orange peel is considered one of the largest volume lignocellulosic residues worldwide, whose chemical constitution makes it a material with great potential for recovery (Tovar *et al.*, 2019; Battista *et al.*, 2020). Agroindustrial residues have the advantages of being abundant in nature, and their use could be adjusted to the principles of green chemistry (Castro *et al.*, 2011). Activated carbon is a material with appreciable surface area, well-developed porosity, and high degree of surface reactivity that can be produced from bituminous coal (Hsu *et al.*, 2000), petroleum coke (Kawano *et al.*, 2008), lignite (Navarro *et al.*, 2006) and lignocellulosic residues (Hassan *et al.*, 2019). Due to its low cost, low toxicity, and high abundance, activated carbon produced from lignocellulosic waste is considered as a green alternative that plays an important role in solving the problem of waste disposal and environmental protection (Battista *et al.*, 2021).

Pandiarajan *et al.* (2018) reported the preparation of activated carbon from shell of orange by chemical activation with KOH and subsequent pyrolysis in a nitrogen atmosphere at 700 °C for 2 h. The solid exhibited a specific surface area (BET) of 592.5 m²/g, while the diameter and pore volume were 1.301 nm and 0.242 ml/g, respectively. Bediako *et al.* (2020) reported the synthesis of activated carbon from orange peel and the effect of activation by KOH, ZnCl₂ and pyrolyzed at 800 °C; it was found that the ZnCl₂-AC exhibited a higher degree of micro-porosity and BET surface area than the KOH-AC with values of 1439.50 and 1370.76 m²/g, respectively. Pan *et al.* (2021) reported the first study of prepared sulfonated carbon derived from orange peel in the esterification of oleic acid with methanol and of citric acid with *n*-butanol; it was reported that the time has a great influence on the BET surface area of materials. When the sulfonation time increases from 10 min to 4 h, the BET surface area decreases from 6.16 to 1.84 m²/g and the pore diameter increases from 22.02 to 44.66 nm. When the sulfonation time was 2 h, the maximum conversion of oleic acid (92.8 %) and citric acid (81.3 %) was obtained. Wang *et al.* (2016) reported the synthesis of porous carbon nanosheets (PCNs) using Zn₅(OH)₈(NO₃)₂·2H₂O as a source of zinc and template and gallic acid as carbon precursor. The obtained nanosheets porous carbon with large surface area (1138 m²/g) and surface groups that make it an ideal candidate for energy storage applications. Xi *et al.* (2021) reported

three-dimensional porous carbon with abundant mesopores by activating lignin from the corn stalks bio-refinery residue with ZnCO_3 , and the resulting carbon had excellent lithium storage performance. Rezaee *et al.* (2008) used activated carbon prepared from almond shell impregnated with ZnSO_4 in nitrate removal. Santosh *et al.* (2021) reported the synthesis of an ecological nano-adsorbent activated with zinc chloride from food residues for the removal of contaminants from biodiesel wash water; the samples were calcined at 350 °C for 3 h and then activated with zinc chloride for 2 h at 500-600 °C. The synthesis of heterostructured ZnS-ZnO/graphene nano-photocatalysts has been reported (Lonkar *et al.*, 2018), from a solid-state mixture of graphite oxide (GO), Zn salt and elemental sulfur by ball milling followed by heat treatment; obtaining hybrids formed by ZnS-ZnO nanoparticles uniformly distributed within the thermally reduced GO (graphene) matrix.

Isomerization of α -pinene epoxide is an important transformation for obtaining compounds of interest in fragrances and compounds with biological activity (Vrbková *et al.*, 2020). There are several reports related to the isomerization of α -pinene oxide using heterogeneous catalytic systems (Stekrova *et al.*, 2014; Sánchez *et al.*, 2019; Singh *et al.*, 2022). The highest selectivity towards campholenic aldehyde (96 %) at total conversion (100 %) was obtained over Ti-MCM-22 at 70 °C using toluene as solvent (Stekrova *et al.*, 2018). There are very few reports in the literature that show α -pinene oxide isomerization over carbon type catalysts. Singh *et al.* (2020) reported the use of carbon spheres from sucrose functionalized with phosphonate groups, for the isomerization of α -pinene oxide; this solid showed 100 % conversion with 22 % selectivity towards campholenic aldehyde (1 h, 160 °C) in the presence of N,N-dimethylformamide. Advani *et al.* (2019) reported that a bio-derived sulfonated carbon catalyst showed excellent performance for the isomerization of α -pinene.

The objective of this work was to evaluate the isomerization of α -pinene epoxide to campholenic aldehyde using a catalyst obtained from orange peels (*Citrus sinensis*). ZnO-ZnS-C material was obtained by activation of orange peel with $\text{ZnSO}_4 \cdot 7\text{H}_2\text{O}$ followed by thermal treatment at 500 °C; furthermore, another solid was synthesized by thermal treatment of orange peel without using activating agent. The obtained materials were characterized through thermogravimetric analysis (TGA), differential thermogravimetric analysis (DTG), X-ray diffraction (XRD), physical adsorption of nitrogen, scanning electron microscopy with energy dispersive X-ray spectroscopy (SEM-EDX), temperature-programmed desorption of ammonia (TPD-NH₃). The materials were used for α -pinene oxide isomerization

Materials and Methods

Preparation of the solid ZnO-ZnS-C

The ZnO-ZnS-C material was prepared by a modification of the procedure reported by Wang *et al.* (2019). The orange (*Citrus sinensis*) peels were washed with water and dried with absorbent paper. Subsequently, they were dried at 80 °C for 24 h and pulverized. After microwave pretreatment, the fine powder obtained was mixed with 20 ml of water and subjected to microwave heating (Mars 5, CEM) from room temperature to 50 °C, keeping the temperature constant for 3 min. Once the orange peel residue was separated from the aqueous phase, it was treated with a solution of $\text{ZnSO}_4 \cdot 7\text{H}_2\text{O}$ (1.4 M) in a weight ratio of activator/peel of 2:1, and the system was kept under stirring at 600 rpm at room temperature for 24 h. For comparison, a carbon was prepared from orange peels only with heat treatment at 500 °C for 1 h in a nitrogen atmosphere at 100 ml/min. The samples obtained were labeled as OAC-Zn (orange peel activated with $\text{ZnSO}_4 \cdot 7\text{H}_2\text{O}$), OC-500 (orange peel without activation).

Characterization

The proximal analysis of the materials was carried out using a thermogravimetric analyzer (SDT-Q600, TA Instruments). The XRD patterns of the samples were recorded using an X-ray diffractometer (Philips, X'pert) with Cu-K α radiation ($\lambda = 0.1542$ nm), in a diffraction angle range of 2θ from 10 to 80 ° in steps of 0.02 °/sec. Surface and textural properties of activated carbon were determined from adsorption-desorption isotherms using nitrogen as adsorbate (ASAP 2020 PLUS, Micromeritics). Scanning electron microscopy (JEOL JSM 6490 LV) was used to investigate the morphology of activated carbon; the elemental composition was identified by EDX (INCA PentaFETx3 Oxford Instruments). Samples were fixed on graphite ribbon, plated with gold, and analyzed in a high-vacuum scanning electron microscope operating at 20 kV. TPD-NH₃ analysis (AutoChem II 2920, Micromeritics) was carried out up to 600 °C by pretreating the samples at 400 °C for 50 min with He (80 ml/min).

α -pinene oxide isomerization

The catalytic tests were performed according to the methodology reported by Sanchez *et al.* (2019) using activated carbons from orange peel with a particle size of 90 μm . Catalysts were mixed with 1 ml of a solution of 0.25 mmol of α -pinene oxide in ethyl acetate. The reaction mixture was heated using a hot plate (Radley tech) at temperatures of 60 $^{\circ}\text{C}$ for 3 h and at 750 rpm. At the end of the reaction, the mixture was centrifuged and a sample was analyzed by Agilent 7890 gas chromatography with FID detector and DB-1 column (30 m \times 320 μm \times 0.5 μm). The products were confirmed by CG-MS.

Results and Discussion

Characterization

The TGA analysis of the OAC-Zn and OC-500 solids are presented in Figures 1a and 1b. The moisture contents of OAC-Zn and OC-500 are 7.8 and 3.0 % w/w, respectively. The volatile matter and ash content increased with the use of the activating agent with values of 16.6 % w/w for the solid without activating agent up to 26.3 % w/w for the solid with activating agent. The fixed carbon content decreased from 70.0 to 26.5 % w/w for the solid OC-500 and OAC-Zn, respectively; this shows that $\text{ZnSO}_4 \cdot 7\text{H}_2\text{O}$ significantly inhibited the release of volatiles, which was consistent with studies reported by Andas *et al.* (2018). In N_2 atmosphere, the initial weight loss occurs between 31 and 120 $^{\circ}\text{C}$ that could be attributed to water loss and the second stage at 120-800 $^{\circ}\text{C}$ may be associated with the decomposition reactions of the organic compounds that have remained after the pyrolysis of the orange peel at 500 $^{\circ}\text{C}$.

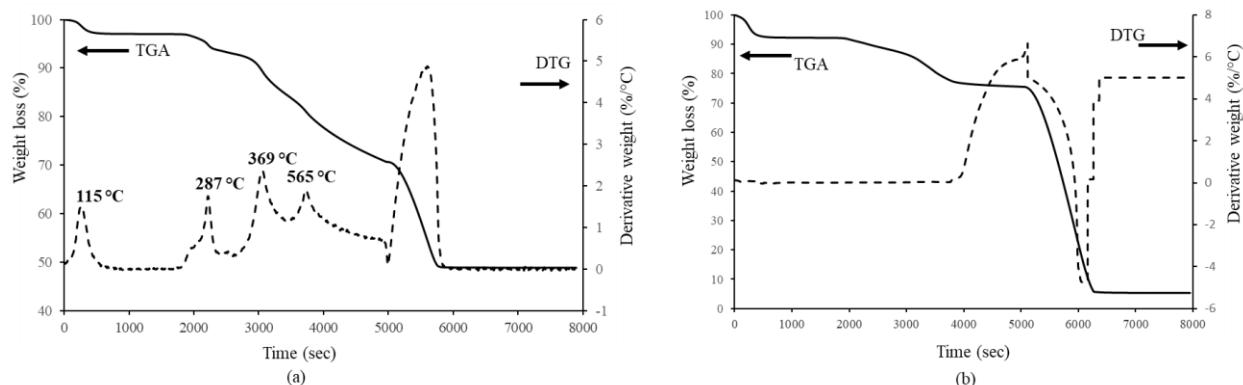


Figure 1. Thermogravimetric analysis (TGA) curves and differential thermogravimetric analysis (DTG) curves of (a) OAC-Zn (orange peel activated with $\text{ZnSO}_4 \cdot 7\text{H}_2\text{O}$) and (b) OC-500 (orange peel without activating agent).

The differences found between Figures 1a and 1b seem to indicate that the presence of $\text{ZnSO}_4 \cdot 7\text{H}_2\text{O}$ has a significant effect on the thermal behavior of orange peel. The curves showed the loss of water up to 140 $^{\circ}\text{C}$, between 143-800 $^{\circ}\text{C}$ there was a stage of significant weight loss, showing that the material still contained thermolabile and abundant substances. These results suggest that the addition of $\text{ZnSO}_4 \cdot 7\text{H}_2\text{O}$ significantly inhibited the release of volatiles (Andas *et al.*, 2018). From the DTG, four peaks are observed; the first peak (84-115 $^{\circ}\text{C}$) is attributed to moisture evaporation and the other three peaks (212-287, 369-385 and 565-587 $^{\circ}\text{C}$) are related to mass loss, which according to Ozdemir *et al.* (2014) would be associated with the decomposition of hemicellulose, cellulose, and lignin.

The crystal structures of the ZnO-ZnS-C compounds were studied by XRD (Figure 2). Figures 2a and 2b show the diffraction patterns corresponding to OAC-Zn and OC-500, respectively. For solid OAC-Zn, signals are observed at approximately $2\theta = 32, 34, 37, 47, 57, 63, 67, 68, 69^{\circ}$ (PDF 98-006-7848), which may be attributed to ZnO in the carbon structure (Pelech *et al.*, 2021). In addition, low intensity signals are observed in the diffraction pattern at $2\theta = 28.5, 47.5, 56.3^{\circ}$ that correspond to the diffraction peaks (220) and (311) of ZnS, respectively (Ghaedi *et al.*, 2012). This result indicates that during the thermal treatment the solid $\text{ZnSO}_4 \cdot 7\text{H}_2\text{O}$ impregnated in orange peel is transformed into ZnO-ZnS. The presence of ZnO was reported in the synthesis of an ecological

nanoadsorbent activated with zinc chloride from food residues (Santosh *et al.*, 2021). The diffraction pattern of the solid OC-500 shows a broad peak corresponding to the diffraction of the C (002) plane at an angle of 2θ from 10 to 30° , which is attributed to sheets of randomly oriented non-graphitic carbon, while the weak diffraction peak from 35 to 50° is due to the C (100) of crystalline graphite (Wei *et al.*, 2019). The absence of sharp peaks in the diffraction pattern indicates the amorphous structure of activated carbons and suggests a limited degree of graphitization (Li *et al.*, 2016).

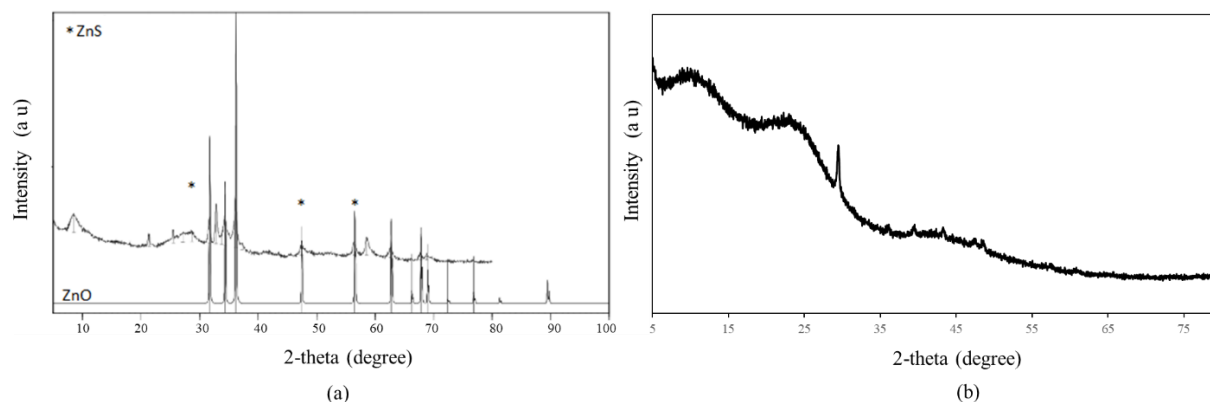


Figure 2. X-ray diffraction (XRD) patterns of: (a) OAC-Zn (orange peel activated with $\text{ZnSO}_4 \cdot 7\text{H}_2\text{O}$) and (b) OC-500 (orange peel without activating agent).

Nitrogen adsorption-desorption isotherms at 77 K were used to investigate the porosity, total pore volume, mean pore diameter, and surface area of OAC-Zn and OC-500. Figure 3a shows the nitrogen adsorption-desorption isotherms at 77 K for OAC-Zn and OC-500. It is clear that the shape of the isotherms changes gradually with the activating agent. The gradual increase in nitrogen adsorption and the larger adsorbed volume (higher horizontal plateau) suggests that additional pores were created and small pores were widened. Furthermore, the increase in nitrogen adsorption is maintained over the entire pressure range, so that the isotherms take a shape resembling a combination of type I and IV with a hysteresis loop suggesting a mixed microporous and mesoporous structure. The pore size distribution curves of OAC-Zn and OC-500 are shown in Figure 3b, confirming the mesoporosity in the material than contains Zn (Poleo *et al.*, 2016). It was observed that the activating agent influenced the porosity of the resulting activated carbon not only creates more new pores, but also widens the pores, thus both contributions cause the development of mesoporosity. It can be seen in Figure 3a that sample OC-500 shows the type I adsorption isotherm, characteristic of microporous materials. The pore size distribution shown in Figure 3b confirms the presence of micropores with size of approximately 1 nm, with the presence of some narrow mesopores (~ 2.5 nm).

Table 1 presents the porosity parameters of the carbon samples. It is evident that the BET surface area (S_{BET}) increases with the addition of $\text{ZnSO}_4 \cdot 7\text{H}_2\text{O}$ from 26 to $157 \text{ m}^2/\text{g}$ for OC-500 and OAC-Zn, respectively; a similar comparison applies in the case of the pore volume. It is important to point out that the pore size distribution of the samples prepared in this study is very narrow and also the value of the mean pore diameter exceeds the reported values for carbons obtained from biomass (Fernández *et al.*, 2014; Ajay *et al.*, 2021), which are between 2 and 5 nm.

Table 1. Physicochemical properties of OAC-Zn and OC-500.

Sample	$S_{\text{BET}} (\text{m}^2/\text{g})$	Pore volume (cm^3/g)	Pore diameter (nm)
OAC-Zn	157	0.180	15
OC-500	26	0.018	1

OAC-Zn: orange peel activated with $\text{ZnSO}_4 \cdot 7\text{H}_2\text{O}$, OC-500: orange peel without activating agent, S_{BET} : BET surface area.

Differences in the morphology of the synthesized activated carbons were identified by SEM analysis, Figure 4. The OAC-Zn material (Figure 4a) presents a smoother morphology with a more uniform distribution of pores. Sample without activating agent (Figure 4b) shows the rough and irregular surface constituted by intercalated thin plates or sheets. This could be explained considering that the thermal treatment favored the expulsion of volatile

matter during the carbonization stage. The release of these elements from the carbonized surface could result in the formation of a rigid carbon skeleton (Pathak *et al.*, 2017). The analysis of the constituent elements was performed by EDX. The spectrum of the OAC-Zn solid (Figure 4a) is mainly formed by Zn (73.7 % w/w), O and C; S and Ca are in lower amount. For the material OC-500 (Figure 4b), C and O are in larger amount than Mg, K and Ca. Furthermore, mapping of Zn and S in the OAC-Zn sample (Figure 4a) showed a uniform distribution of carbon-supported ZnO-ZnS species. The results of the EDX analysis agree with the diffraction patterns, indicating the formation of ZnO-ZnS and carbon.

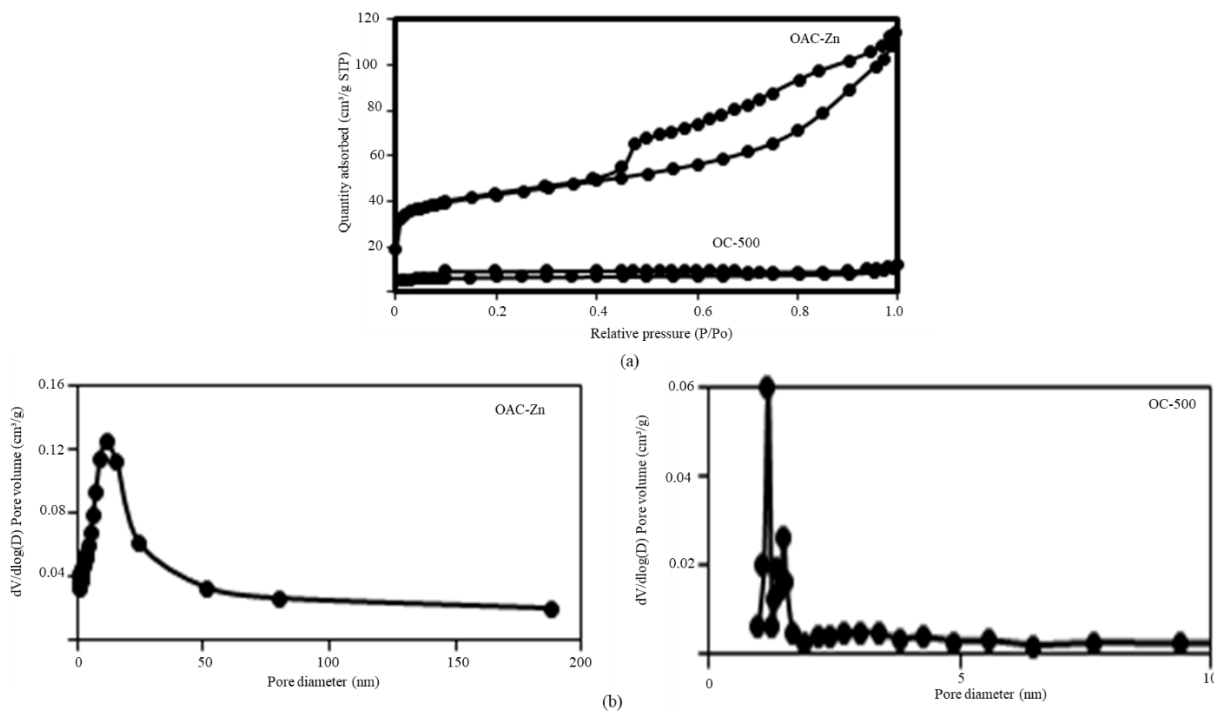


Figure 3. (a) Nitrogen adsorption-desorption isotherms and (b) pore size distribution of: OAC-Zn (orange peel activated with $\text{ZnSO}_4 \cdot 7\text{H}_2\text{O}$) and OC-500 (orange peel without activating agent).

The acid properties in terms of density and strength of sites were studied by TPD- NH_3 . Figures 5a and 5b show the ammonia thermograms for the obtained carbon materials. It was observed that the carbon obtained from orange peel activated with $\text{ZnSO}_4 \cdot 7\text{H}_2\text{O}$ exhibits acidity in the temperature range between 100 and 450 °C, which would correspond to physisorbed NH_3 low and medium strength acid sites. The signal that appears with a maximum at a temperature of 550 °C can be attributed to carbon decomposition in correspondence with the TGA results.

The solid OC-500 coming from only the thermal treatment shows three low intensity signals, the first with a maximum at 180 °C that can be assigned to physisorbed ammonia or low strength acid sites; the second signal with maxima at 410 °C can be assigned to medium strength acid sites and the third at 550 °C could correspond to carbon decomposition products. From this result is possible to infer that both solids have acid sites with the necessary strength to catalyze the isomerization of α -pinene oxide (Barakov *et al.*, 2022).

α -pinene oxide isomerization

From isomerization of α -pinene oxide the observed products were: campholenic aldehyde (CA) carveol (C) and cymene (Cy), Table 2. The results show that the highest conversion was obtained over the carbon from the orange peel activated with $\text{ZnSO}_4 \cdot 7\text{H}_2\text{O}$. This result is not surprising due to the presence of mesopores and a larger surface area of this solid, which offers greater accessibility and facilitates the diffusion of the molecules through the internal surface to the available active centers of the catalyst where the substrate transformation reactions would take place; furthermore, the presence of Zn favors the presence of Lewis acid sites that are required for α -pinene isomerization into campholenic aldehyde. For the OAC-Zn catalyst, an increase in the conversion is observed from

loadings of 25 to 90 mg at 24 h with conversion increase from 41 to 79 %. While a decrease was observed in the selectivity towards campholenic aldehyde from 96 to 56 % and an increase in the selectivity towards carveol from 0 to 41 %.

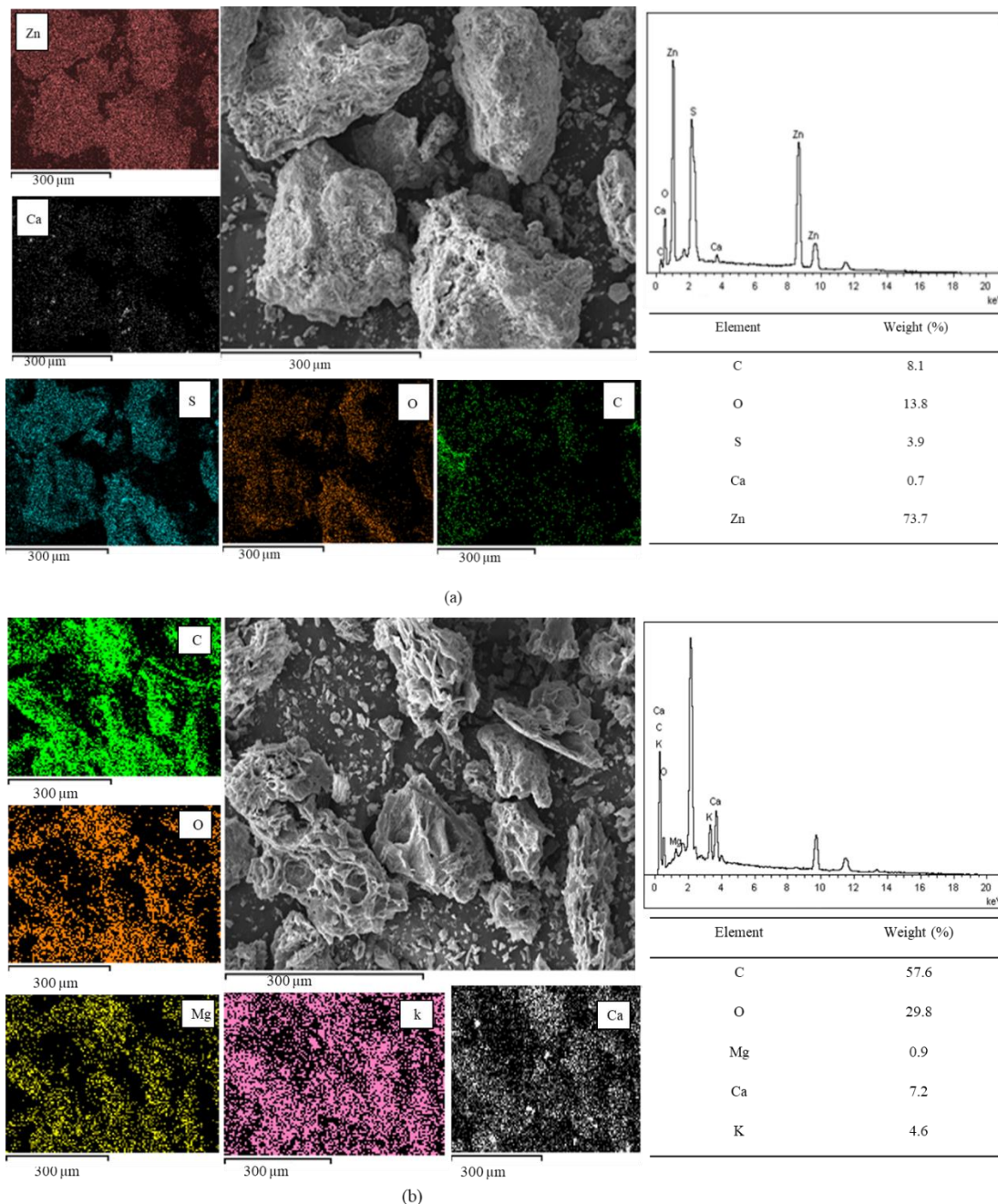


Figure 4. Scanning electron microscopy with energy dispersive X-ray spectroscopy (SEM-EDX) analysis and elemental mapping of: (a) OAC-Zn (orange peel activated with $ZnSO_4 \cdot 7H_2O$) and (b) OC-500 (orange peel without activating agent).

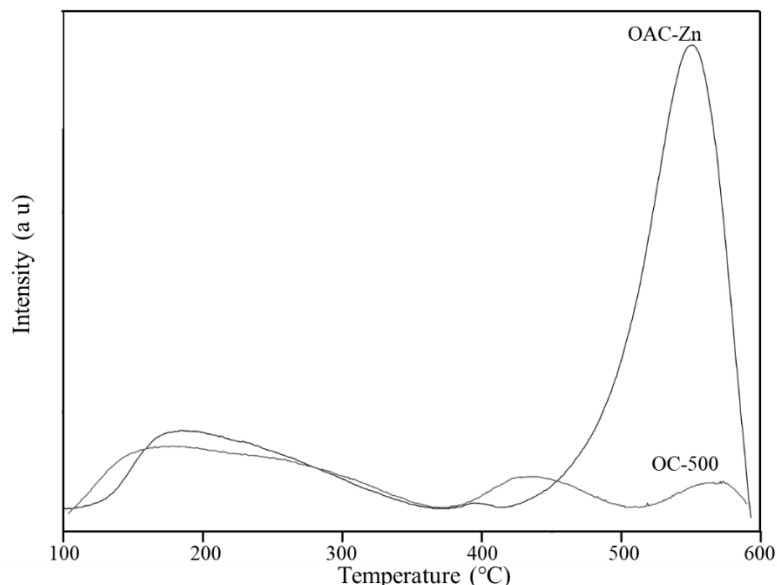


Figure 5. Temperature-programmed desorption of ammonia (TPD-NH₃) of OAC-Zn (orange peel activated with ZnSO₄·7H₂O) and OC-500 (orange peel without activating agent).

Table 2. Conversion and selectivity over synthesized solids from orange peel.

Catalyst (mg)	Time (h)	Conversion (%)	Selectivity (%)		
			CA	C	Cy
OAC-Zn (50)	3	27	97	0	3
OAC-Zn (25)	24	41	96	0	4
OAC-Zn (50)	24	61	77	19	4
OAC-Zn (75)	24	68	76	24	0
OAC-Zn (90)	24	79	56	41	3
OC-500 (75)	24	0	0	0	0

Reaction conditions: 60 °C, 750 rpm, 0.25 mmol α -pinene oxide; CA: campholenic aldehyde; C: carveol; Cy: cymene; OAC-Zn: orange peel activated with ZnSO₄·7H₂O; OC-500: orange peel without activating agent.

Apparently, an increase in the number of active sites favors the reactions that lead to the formation of carveol. These results are different from those reported in the literature by Advani *et al.* (2020) and Singh *et al.* (2020) for carbon catalysts where carveol selectivity predominates. For a constant OAC-Zn loading, the conversion increased with an increase in reaction time and it reached 61 % at 24 h. However, the selectivity towards campholenic aldehyde decreased from 97 to 77 % while the selectivity towards carveol increases. A longer contact time between α -pinene oxide molecules and the active center of the catalyst favors the formation of other reaction products from campholenic aldehyde or carveol. The effect of reaction time (1-5 h) was studied by Sighn *et al.* (2022) for α -pinene oxide isomerization over zirconium phosphate catalysts, reporting an increase of conversion from 43 to 100 % and selectivity to *trans*-carveol from 69 to 73 %; with a selectivity towards campholenic aldehyde of around 20 %.

Figure 6 shows the proposed reaction pathway for the formation of campholenic aldehyde and carveol from the isomerization reaction of α -pinene oxide over the tested catalyst. The initial formation of a very stable tertiary carbocation is proposed through the coordination of the substrate with the Lewis sites of the solid (Zn); subsequently, the carbocation rearranges generating campholenic aldehyde and carveol (Pitúnová-Štekrová *et al.*, 2018).

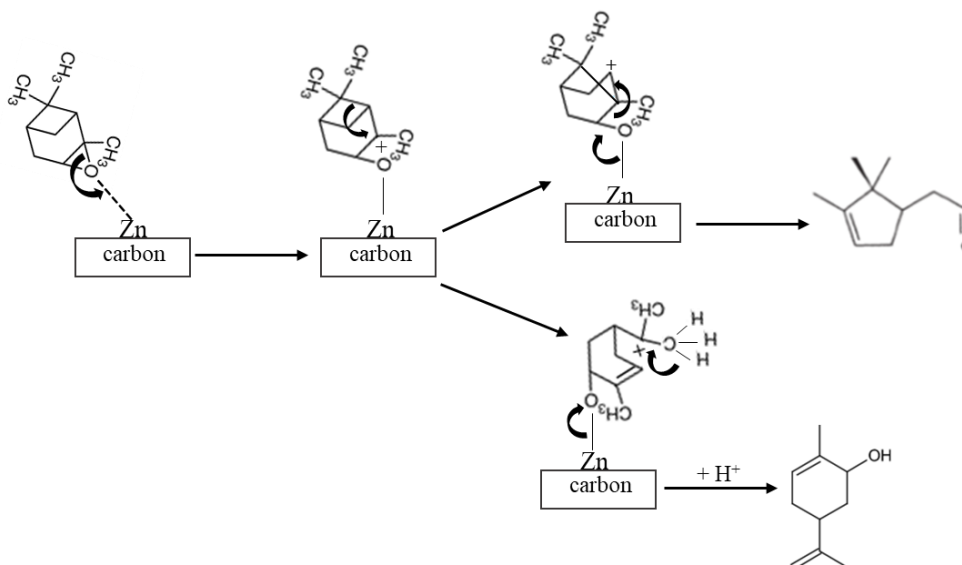


Figure 6. Proposed reaction pathway of product formation in the isomerization of α -pinene oxide.

Conclusions

Campholenic aldehyde was synthesized over a carbonaceous material obtained from orange peels using $ZnSO_4 \cdot 7H_2O$ as activating agent. The solid obtained without using activating agent that showed microporosity was not active for campholenic aldehyde synthesis; while the OAC-Zn material that presented mesoporosity, acidity and zinc species showed a good α -pinene epoxide conversion and high selectivity to campholenic aldehyde.

Acknowledgements

The authors acknowledge the financial support from Universidad de Antioquia (UdeA). M.M-Q. acknowledges to the International Institute of Education (IIE-SRF) and the “Fondo de apoyo a la internacionalización de la investigación-CODI (UdeA)”.

References

- Advani, J. H., Singh, S. A., Noor-ul, H. K., Hari, C. B., Biradar, A. V. (2020). Black yet green: sulfonic acid functionalized carbon as an efficient catalyst for highly selective isomerization of α -pinene oxide to trans-carveol. *Applied Catalysis B: Environmental*, 268, 118456.
- Ajay, K. M., Dinesh, M. N., Byatarayappa, G., Radhika, M. G., Kathyayini, N., Vijeth, H. (2021). Electrochemical investigations on low cost KOH activated carbon derived from orange-peel and polyaniline for hybrid supercapacitors. *Inorganic Chemistry Communications*, 127, 108523.
- Andas, J., Ab, N. A. (2018). Synthesis and characterization of tamarind seed activated carbon using different types of activating agents: a comparison study. *Materials Today: Proceedings*, 5 (9), 17611-17617.
- Barakov, R., Shcherban, N., Mäki-Arvela, P., Yaremov, P., Bezverkhyy, I., Wärnå, J., Murzin, D. J. (2022). Hierarchical beta zeolites as catalysts in α -pinene oxide isomerization. *ACS Sustainable Chemistry & Engineering*, 10(20), 6642-6656.
- Battista, A., Muhammad, H. H., Zaman, W. Q., Mohsin, M. Z., Zhang, J., Liu, Z., Tian, X., Rehman, S-ur., Khan, I. M., Niazi, S., Zhuang, Y., Guo, M. (2021). Advances in sustainable approaches utilizing orange peel waste to produce highly value-added bioproducts. *Critical Reviews in Biotechnology*, 42(8), 1284-1303.

- Battista, F., Remelli, G., Zanzoni, S., Bolzonella, D. (2020). Valorisation of residual orange peels: limonene recovery, volatile fatty acids and biogas productions. *ACS Sustainable Chemistry*, 8(1), 6834–6843.
- Fernandez, M. E., Nunell, G. V., Bonelli, P. R., Cukierman, A. L. (2014). Activated carbon developed from orange peels: batch and dynamic competitive adsorption of basic dyes. *Industrial Crops and Products*, 62, 437-445.
- Ghaedi, M., Larki, H. A., Kokhdan, S. N., Marahel, F., Sahraei, R., Daneshfar, A., Purkait, M. K. (2012). Synthesis and characterization of zinc sulfide nanoparticles loaded on activated carbon for the removal of methylene blue. *Environmental Progress & Sustainable Energy*, 32(3), 535-542.
- Hassan, M. F., Sabri, M. A., Fazal, H., Hafeez, A., Shahzad, N., Hussain, M. (2019). Recent trends in activated carbon fibers production from various precursors and applications—A comparative review. *Journal of Analytical and Applied Pyrolysis*, 145, 104715-10479.
- Hsu, L-Y., Teng, H. (2000) Influence of different chemical reagents on the preparation of activated carbons from bituminous coal. *Fuel Processing Technology*, 64(1-3), 155-166.
- Kawano, T., Kubota, M., Onyango, M. S., Watanabe, F., Matsuda, H. (2008). Preparation of activated carbon from petroleum coke by KOH chemical activation for adsorption heat pump. *Applied Thermal Engineering*, 28 (8-9), 865-871.
- Li, Z., Zhai, K., Wang, G., Li, Q., Guo, P. (2016). Preparation and electrocapacitive properties of hierarchical porous carbons based on loofah sponge. *Materials*, 9(11), 912-922.
- Lonkar, S. P., Pillai, V. V., Alhassan, S. M. (2018). Facile and scalable production of heterostructured ZnS-ZnO/Graphene nano-photocatalysts for environmental remediation. *Scientific Reports*, 8(1), 13401-13414.
- Muniandy, L., Adam, F., Mohamed, A. R., Ng, E. P. (2014). The synthesis and characterization of high purity mixed microporous/mesoporous activated carbon from rice husk using chemical activation with NaOH and KOH. *Microporous and Mesoporous Materials*, 197, 316-323.
- Ozdemir, I., Şahin, M., Orhan, R., Erdem, M. (2014). Preparation and characterization of activated carbon from grape stalk by zinc chloride activation. *Fuel Processing Technology*, 125, 200-206.
- Pajaro, N. P., Oliver, V., Tadeo, J. (2011). Química verde: un nuevo reto. *Ciencia e Ingeniería Neogranadina*, 21(2), 169-182.
- Pandiarajan, A., Kamaraj, R., Vasudevan, S., Vasudevan, S. (2018). OPAC (orange peel activated carbon) derived from waste orange peel for the adsorption of chlorophenoxyacetic acid herbicides from water: Adsorption isotherm, kinetic modelling and thermodynamic studies. *Bioresource Technology*, 261, 329-341.
- Pathak, P. D., Mandavgane, A. S., Kulkarni, B. D. (2017). Fruit peel waste: characterization and its potential uses. *Current Science*, 113(3), 444-454.
- Pełech, I., Sibera, D., Staciwa, P., Kusiak-Nejman, E., Kapica-Kozar, J., Wanag, A., Narkiewicz, U., Morawski, A. W. (2021). ZnO/carbon spheres with excellent regenerability for post-combustion CO₂ capture. *Materials*, 14(21), 6478-6487.
- Pitínová-Štekrová, M., Eliášová, P., Weissenberger, T., Shamzhy, M., Musilová, Z., Čejka, J. (2018). Highly selective synthesis of campholenic aldehyde over Ti-MWW catalysts by α -pinene oxide isomerization. *Catalysis Science & Technology*, 8(18), 4690-4701.
- Poleo, N., Oliveros, S., Colina M., Rincón, N., Mesa, J., Colina, G. (2010). Study of different chemical activations on obtaining activated carbon from *Hymenaea courbaril* L. shell for cadmium (II) removal. *Revista Técnica de la Facultad de Ingeniería de la Universidad Zulia*, 33(1), 29-38.
- Rezae, A., Godini, H., Dehestani, S., Khavanin, A. (2008). Application of impregnated almond shell activated carbon by zinc and zinc sulfate for nitrate removal from water. *Journal of Environmental Health Science & Engineering*, 5(2), 125-130.
- Sánchez, J. E., Villa, A. L. (2019). Isomerization of α and β pinene epoxides over Fe or Cu supported MCM-41 and SBA-15 materials. *Applied Catalysis A: General*, 580, 17-27.

- Sánchez, J. E., Gelves, J. F., Márquez, M. A., Dorkis, L., Villa, A. L. (2020). Catalytic isomerization of α -pinene epoxide over a natural zeolite. *Catalysis Letters*, 150, 3132-3148.
- Santhosh, A., Dawn, S. S. (2021). Synthesis of zinc chloride activated eco-friendly nano-adsorbent (activated carbon) from food waste for removal of pollutant from biodiesel wash water. *Water Science Technology*, 84(5), 1170-1181.
- Singh, S. A., Advani, J. H., Biradar, A. V. (2020). Phosphonate functionalized carbon to trans-carveol. *Dalton Transactions*, 49, 7210-7217.
- Singh, A. S., Naikwadi, D. R., Ravi, K., Biradar, A. V. (2022). Chemoselective isomerization of α -pinene oxide to trans- by robust and mild Brønsted acidic zirconium phosphate catalyst. *Molecular Catalysis*, 521, 112189.
- Sneha, D., Thorat, P. V., Topare, N. S. (2018). Preparation and characterization of activated carbon from orange peels. *Journal of Catalyst and Catalysis*, 5(1), 15-20.
- Štekrová, M., Kumar, N., Aho, A., Sinev, I., Grunert, W., Dahl, J., Roine, J., Arzumanov, S. S., Mäki-Arvela, P., Murzin, D. Y. (2014). Isomerization of α -pinene oxide using Fe-supported catalysts: selective synthesis of campholenic aldehyde. *Applied Catalysis A: General*, 470, 162-176.
- Stekrova, M., Eliášová, P., Weissenberger, T., Shamzhy, M., Musilova, Z., Cejka, J. (2018). Highly selective synthesis of campholenic aldehyde over Ti-MWW catalysts by α -pinene oxide isomerization. *Journal Catalysis Science Technology*, 8, 4690-4701.
- Tovar, A. K., Godínez, L. A., Espejel, F., Ramírez-Zamora, R. M., Robles, I. (2019). Optimization of the integral valorization process for orange peel waste using a design of experiments approach: production of high-quality pectin and activated carbon. *Waste Management*, 85, 202-213.
- Vrbková, E., Vyskočilová, E., Lhotka, M., Červený, L. (2020). Solvent influence on selectivity in α -pinene oxide isomerization using MoO₃-modified zeolite BETA. *Catalysts*, 10(11), 1244-1261.
- Wang, L., Zhou, P., Guo, Y., Zhang, J., Qiu, X., Guan, Y., Yu, M., Zhue, H., Zhang, Q. (2019). The effect of ZnCl₂ activation on microwave absorbing performance in walnut shell-derived nano-porous carbon. *RSC Advances*, 9(17), 9718-9728.
- Wang, Y., Dou, H., Ding, B., Wang, J., Chang, Z., Xu, Y. L., Hao, X. D. (2016). Nanospace-confined synthesis of oriented porous carbon nanosheets for high-performance electrical double layer capacitors. *Journal of Materials Chemistry A*, 4(43), 16879-16885.
- Wei, Q., Chen, Z., Cheng, Y., Wang, X., Yang, X., Wang, Z. (2019). Preparation and electrochemical performance of orange peel based-activated carbons activated by different activators. *Colloids and Surfaces A: Physicochemical and Engineering Aspects*, 574, 221-227.
- Xi, Y., Huang, S., Yang, D., Qiu, X., Su, H., Yi, C., Li, Q. (2021). Hierarchical porous carbon derived from the gas-exfoliation activation of lignin for high-energy lithium-ion batteries. *Green Chemistry*, 22(13), 4321-4330.

Editor Asociado: Roger José Solano 

Instituto de Superficies y Catálisis “Prof. Eduardo Choren”, Facultad de Ingeniería,
Universidad del Zulia, Maracaibo, Venezuela
Departamento de Ingeniería Química, Grupo Catalizadores y Adsorbentes,
Universidad de Antioquia - UdeA, Calle 70 No. 52-21. Medellín, Colombia



UNIVERSIDAD
DEL ZULIA

REVISTA TECNICA

DE LA FACULTAD DE INGENIERIA
UNIVERSIDAD DEL ZULIA

Volumen 46. Año 2023, Edición continua _____

*Esta revista fue editada en formato digital y publicada
en abril 2023, por el **Fondo Editorial Serbiluz,**
Universidad del Zulia. Maracaibo-Venezuela*

**www.luz.edu.ve
www.serbi.luz.edu.ve
www.produccioncientificaluz.org**